

# Analysis of underground propagation effects of lightning electromagnetic fields in different geological environments

Yunfeng Zhang, Jialiang Gu\* and Erchun Zhang

*Key Laboratory of Meteorological Disaster, Ministry of Education (KLME), Joint International Research Laboratory of Climate and Environment Change (ILCEC), Collaborative Innovation Center on Forecast and Evaluation of Meteorological Disasters (CIC-FEMD), Key Laboratory for Aerosol-Cloud-Precipitation of China Meteorological Administration, Nanjing University of Information Science & Technology, Nanjing, China;*

*ORCIDs: <http://orcid.org/0000-0002-7945-1239>; <http://orcid.org/0000-0003-0950-8794>;  
<http://orcid.org/0000-0002-5064-1602>*

**Abstract.** Studying underground propagation effects of lightning electromagnetic fields in different geological environments will contribute to more reasonable designs for protecting underground cables and electronic equipment. In this paper, we have analyzed influences of different geological environments, depths and soil water content on underground propagation of lightning electromagnetic fields in detail by using the finite difference time domain (FDTD) method in the 2-D cylindrical coordinate system to calculate components of underground electromagnetic fields at a horizontal distance of 200 m, including vertical electric field  $E_z$ , horizontal electric field  $E_r$  and azimuthal magnetic field  $H_\phi$ . The results show that the underground electric field is predominantly horizontal. Propagation of lightning electromagnetic fields in wet clay and wet limestone environment changes significantly compared to freshwater environment. Attenuation is larger with depth in wet clay and wet limestone, while propagation is unaffected in freshwater. When water content in soils ranges from 5% to 25%, the vertical electric field has the largest attenuation and the azimuthal magnetic field has the least attenuation. The electromagnetic fields in clay are most sensitive to changes in water content.

**Keywords:** FDTD, lightning electromagnetic fields, different geological environments, water content, underground propagation

## 1. Introduction

Propagation effects of lightning electromagnetic fields have direct or indirect impacts on the accuracy of lightning positioning systems, inductive coupling of high-voltage transmission lines, and lightning surge protection. Therefore, many theoretical calculations and practical applications of lightning electromagnetic fields above ground have appeared in early studies. For example, Rubinstein proposed Cooray-Rubinstein algorithm for calculating the horizontal electric field in arbitrary height [1]. Hill and Wait proposed the concept of attenuation functions and developed Cooray-Rubinstein algorithm in frequency domain [2]. Izadi et al. proposed numerical expressions in time domain for calculating lightning electromagnetic fields

---

\*Corresponding author: Jialiang Gu, Nanjing University of Information Science & Technology, Nanjing 210044, China.  
E-mail: 20171202221@nuist.edu.cn.

at close and intermediate distances from lightning channel and validated them by measured data [3]. Baba and Rakov used FDTD method [4] to calculate lightning electromagnetic fields at different distances and lightning surge of overhead transmission lines [5]. Boumaiza et al. proposed a new method based on FDTD method and Kirchhoff's laws to deduce current and voltage induced by a lightning wave in every node of the overhead line directly without using FFT [6].

However, a few systematic studies on underground propagation of lightning electromagnetic fields can be found in the literature due to the complexity of underground environments and difficulties in establishing a more reasonable model and measuring of underground electromagnetic fields. Previous researches were primarily focused on analyzing effects of the ground stratification on underground lightning electromagnetic fields [7–10]. But these studies did not consider effects of changes in geological environments, water content, soil dispersion, and other factors on propagation of underground electromagnetic fields.

In this paper, underground lightning electromagnetic fields are simulated by FDTD method in the 2-D cylindrical coordinate system at a horizontal distance of 200 m. The influences of geological environments, different depths and soil water content on propagation of electromagnetic fields are systematically analyzed. The results presented herein may provide theoretical guidance for protecting underground cables and detecting underground electromagnetic signals.

## 2. Analysis method and computation model

### 2.1. FDTD Method

The FDTD method is used to solve Maxwell's equations by converting partial differential equations into difference equations and performing differential operations [4]. The differential equations for electromagnetic field components in the 2-D cylindrical coordinate system can be written in algebraic iterative equations as follows:

$$E_z^{n+1} \left( i, j + \frac{1}{2} \right) = \frac{2\varepsilon - \sigma\Delta t}{2\varepsilon + \sigma\Delta t} E_z^n \left( i, j + \frac{1}{2} \right) + \frac{2\Delta t}{(2\varepsilon + \sigma\Delta t) r_i \Delta r} \left[ r_{i+(1/2)} H_\varphi^{n+1/2} \left( i + \frac{1}{2}, j + \frac{1}{2} \right) - r_{i-(1/2)} H_\varphi^{n+1/2} \left( i - \frac{1}{2}, j + \frac{1}{2} \right) \right] \quad (1)$$

$$E_r^{n+1} \left( i + \frac{1}{2}, j \right) = \frac{2\varepsilon - \sigma\Delta t}{2\varepsilon + \sigma\Delta t} E_r^n \left( i + \frac{1}{2}, j \right) - \frac{2\Delta t}{(2\varepsilon + \sigma\Delta t) \Delta z} \left[ H_\varphi^{n+1/2} \left( i + \frac{1}{2}, j + \frac{1}{2} \right) - H_\varphi^{n+1/2} \left( i + \frac{1}{2}, j - \frac{1}{2} \right) \right] \quad (2)$$

$$H_\varphi^{n+1/2} \left( i + \frac{1}{2}, j + \frac{1}{2} \right) = H_\varphi^{n-1/2} \left( i + \frac{1}{2}, j + \frac{1}{2} \right) + \frac{\Delta t}{\mu \Delta r} \left[ E_z^n \left( i + 1, j + \frac{1}{2} \right) - E_z^n \left( i, j + \frac{1}{2} \right) \right] - \frac{\Delta t}{\mu \Delta z} \left[ E_r^n \left( i + \frac{1}{2}, j + 1 \right) - E_r^n \left( i + \frac{1}{2}, j \right) \right]. \quad (3)$$

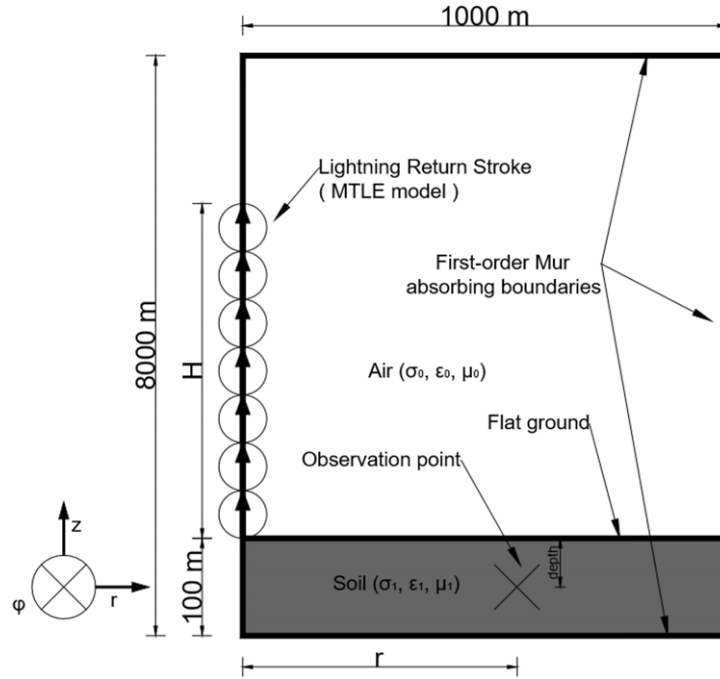


Fig. 1. Schematic diagram of the FDTD simulation domain in the 2-D cylindrical coordinate system.

Where,  $E_r$  is the horizontal electric field,  $E_z$  is the vertical electric field, and  $H_\phi$  is the azimuthal magnetic field,  $\Delta t$  is the time increment, and  $\Delta r$  and  $\Delta z$  are the vertical and horizontal steps in the spatial grid, respectively.

## 2.2. Computation model

The simulation region is shown in Fig. 1. In the figure, the working space of  $1000 \text{ m} \times 8000 \text{ m}$  is divided uniformly into  $1 \text{ m} \times 1 \text{ m}$  square cells, and the time increment is set to  $1.67 \text{ ns}$  in order to fulfill the Courant–Friedrichs–Lewy (CFL) stability criterion [11]. The soil thickness (between the ground surface and the bottom absorbing boundary) is set to  $100 \text{ m}$ , and the channel height  $H$  is set to  $7.5 \text{ km}$ . The upper, bottom, and right-side boundaries are represented by the first-order Mur absorbing boundaries [12] in order to suppress unwanted reflections there in this study. Assuming the channel of the return stroke is a thin, unbranched wire that runs perpendicular to the flat and lossy ground, and the lightning return stroke is represented by the modified transmission-line with exponential current decay (MTLE) model [13], which is simulated in the FDTD computations by a vertical phased-current-source array [14], the electromagnetic field components in a certain horizontal distance  $r$  and depth can be calculated using FDTD method in the cylindrical coordinate system.

In the MTLE model, lightning return stroke current at height  $z$  and time  $t$ ,  $I(z, t)$ , is expressed as follows:

$$\begin{cases} I(z, t) = P(z)I(0, t - z/v) \\ P(z) = e^{-z/\lambda_e} \end{cases} \quad (4)$$

Where,  $P(z)$  is the current attenuation factor,  $\lambda_e = 2000$  is the current attenuation coefficient, and  $v = 1.5 \times 10^8 \text{ m/s}$  is the return stroke speed. Here, the Heidler's function improved by Diendorfer and Uman

Table 1  
Parameters of subsequent return stroke current [16]

$I_{01} / \text{kA}$	$\tau_{11} / \mu\text{s}$	$\tau_{12} / \mu\text{s}$	$n_1$	$I_{02} / \text{kA}$	$\tau_{21} / \mu\text{s}$	$\tau_{22} / \mu\text{s}$	$n_2$
10.7	0.25	2.5	2	6.5	2	230	2

[15], which includes the breakdown current and corona current, is used as the subsequent return stroke current  $I(0, t)$ . It is defined as:

$$\begin{cases} I(0, t) = \frac{I_{01}}{\eta_1} \frac{(t/\tau_{11})^{n_1}}{(t/\tau_{11})^{n_1} + 1} e^{-t/\tau_{12}} + \frac{I_{02}}{\eta_2} \frac{(t/\tau_{21})^{n_2}}{(t/\tau_{21})^{n_2} + 1} e^{-t/\tau_{22}} \\ \eta_1 = e^{-(\tau_{11}/\tau_{12})(n_1 \tau_{12}/\tau_{11})^{1/n_1}} \\ \eta_2 = e^{-(\tau_{21}/\tau_{22})(n_2 \tau_{22}/\tau_{21})^{1/n_2}} \end{cases} \quad (5)$$

Where,  $I_{01}$  and  $I_{02}$  are breakdown and corona current peaks,  $\tau_{11}$  and  $\tau_{21}$  are currents' rise time,  $\tau_{12}$  and  $\tau_{22}$  are currents' fall time,  $n_1$  and  $n_2$  are current steepness factors, and  $\eta_1$  and  $\eta_2$  are current peaks' correction factors, respectively. The parameters corresponding to the subsequent return stroke current used in this paper are shown in Table 1.

### 3. Validation of FDTD method

In order to verify that the FDTD method can effectively be applied to calculate underground electromagnetic fields, here we use analytical formulas in time domain proposed by Cooray [17] to compare it. Although Cooray's analytical formulas simplify Sommerfeld's integrals method, they have been proven to be effective [18,19]. The results calculated by Cooray's analytical formulas and FDTD method are consistent in the same condition, as those are shown in Fig. 2. Therefore, the FDTD method can be used to precisely calculate propagation of underground electromagnetic fields in a certain horizontal distance and depth.

## 4. Influence of geological features

### 4.1. Influence of different environments and depths

In order to explore propagation effects of lightning electromagnetic fields in different geological conditions, three typical environments are considered in this study, including freshwater, wet limestone and wet clay. The electromagnetic parameters of these three environments are listed in Table 2.

Figures 3–5 show the electromagnetic fields in different depths in three different geological environments, which are calculated using FDTD method. One can see that electromagnetic field components in each geological environment have different effects on attenuation with depth.

In freshwater, amplitude and rise time do not change significantly with depth, regardless of the electric field or the magnetic field. Depth has little effect on electromagnetic field propagation, and the energy loss is small. While, attenuation is significant as depth increases in wet limestone and wet clay, regardless of the electric field or the magnetic field. This is because the conductivity of freshwater is much smaller than

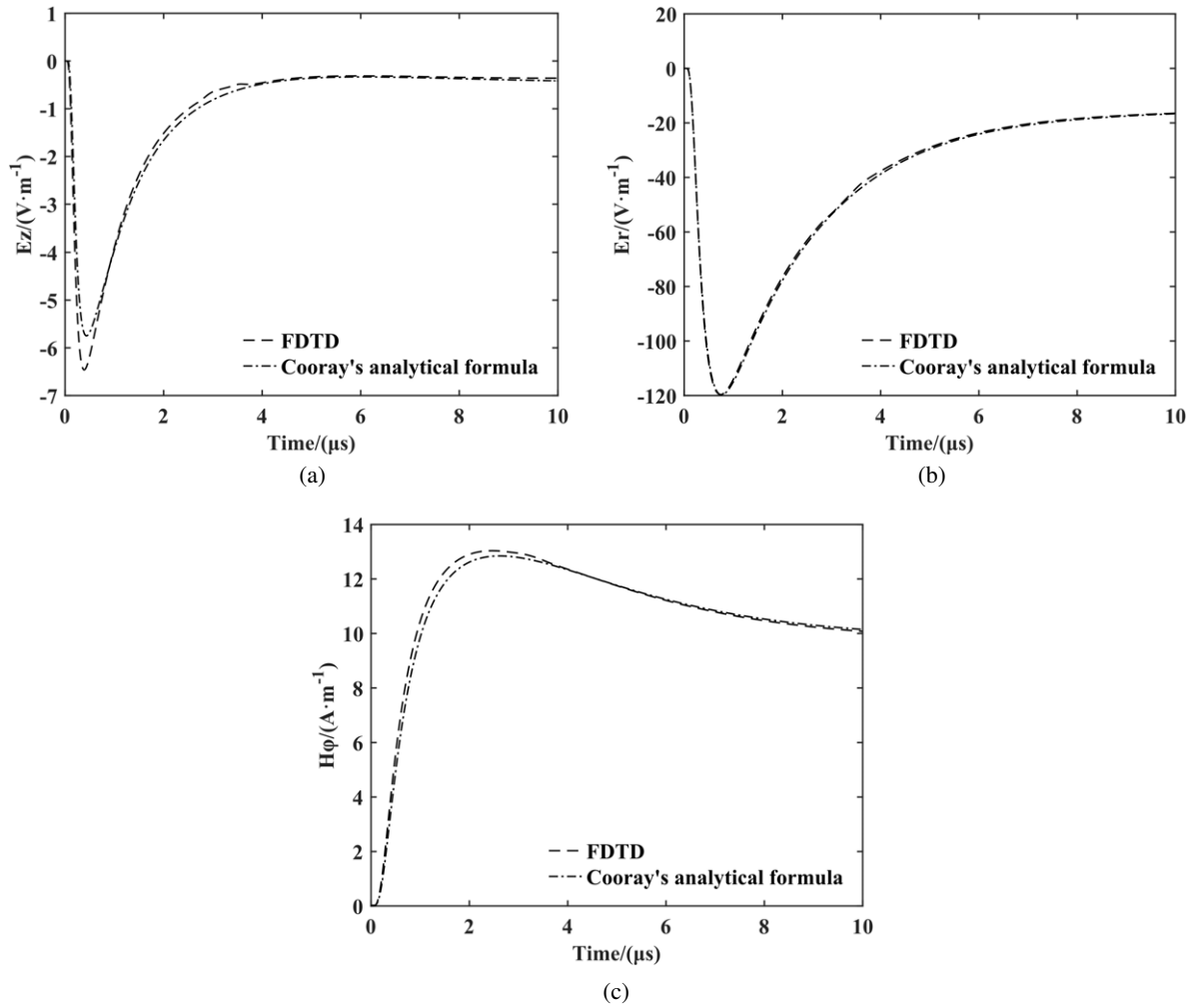


Fig. 2. Underground electromagnetic field components generated by the lightning return stroke in 5 m depth at a horizontal distance of 100 m with the earth conductivity of 0.01 S/m, calculated by FDTD method and Cooray's analytical formulas. (a) Vertical electric field, (b) Horizontal electric field, (c) Azimuthal magnetic field.

Table 2  
Electromagnetic parameters of freshwater, wet limestone and wet clay [20]

Environment	Conductivity (S/m)	Relative permittivity	Relative permeability
Freshwater	$10^{-4}$	81	1
Wet limestone	0.05	8	1
Wet clay	0.1	12	1

that of wet limestone and wet clay. It is known that conductivity is the main factor affecting high-frequency components of electromagnetic waves. The larger the conductivity, the greater the attenuation of the high-frequency components of electromagnetic waves, which leads to weaker penetration of electromagnetic

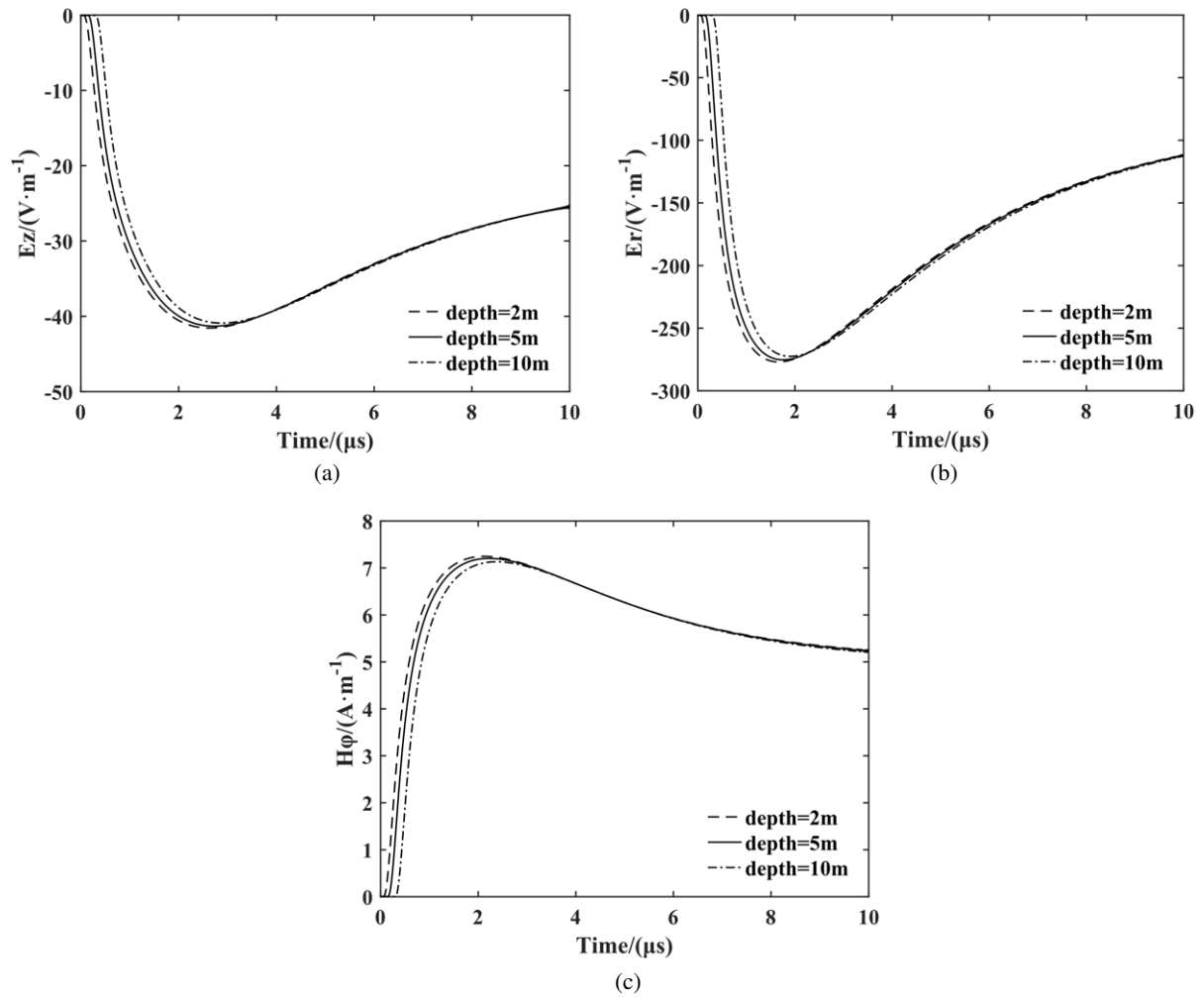


Fig. 3. Electromagnetic field components generated by the lightning return stroke in freshwater in different depths at a horizontal distance of 200 m, simulated using FDTD method. (a) Vertical electric field, (b) Horizontal electric field, (c) Azimuthal magnetic field.

waves and shallower penetration depth. Therefore, the electromagnetic field waveforms in wet limestone and wet clay show more significant changes with depth, including decrease in amplitude and delay in rise time, compared to freshwater.

Moreover, no matter the geology in which the electromagnetic fields propagate, amplitude of the horizontal electric field is far greater than that of the vertical electric field, indicating that the underground electric field is predominantly horizontal.

#### 4.2. Influence of soil water content

Lightning generally occurs during precipitation, and precipitation determines the water content in soil. Soil is a porous medium, and the ion content and solubility of the solution adsorbed in pores will affect ionization of the soil [21], thus changes in water content will determine the soil conductivity. Moreover,

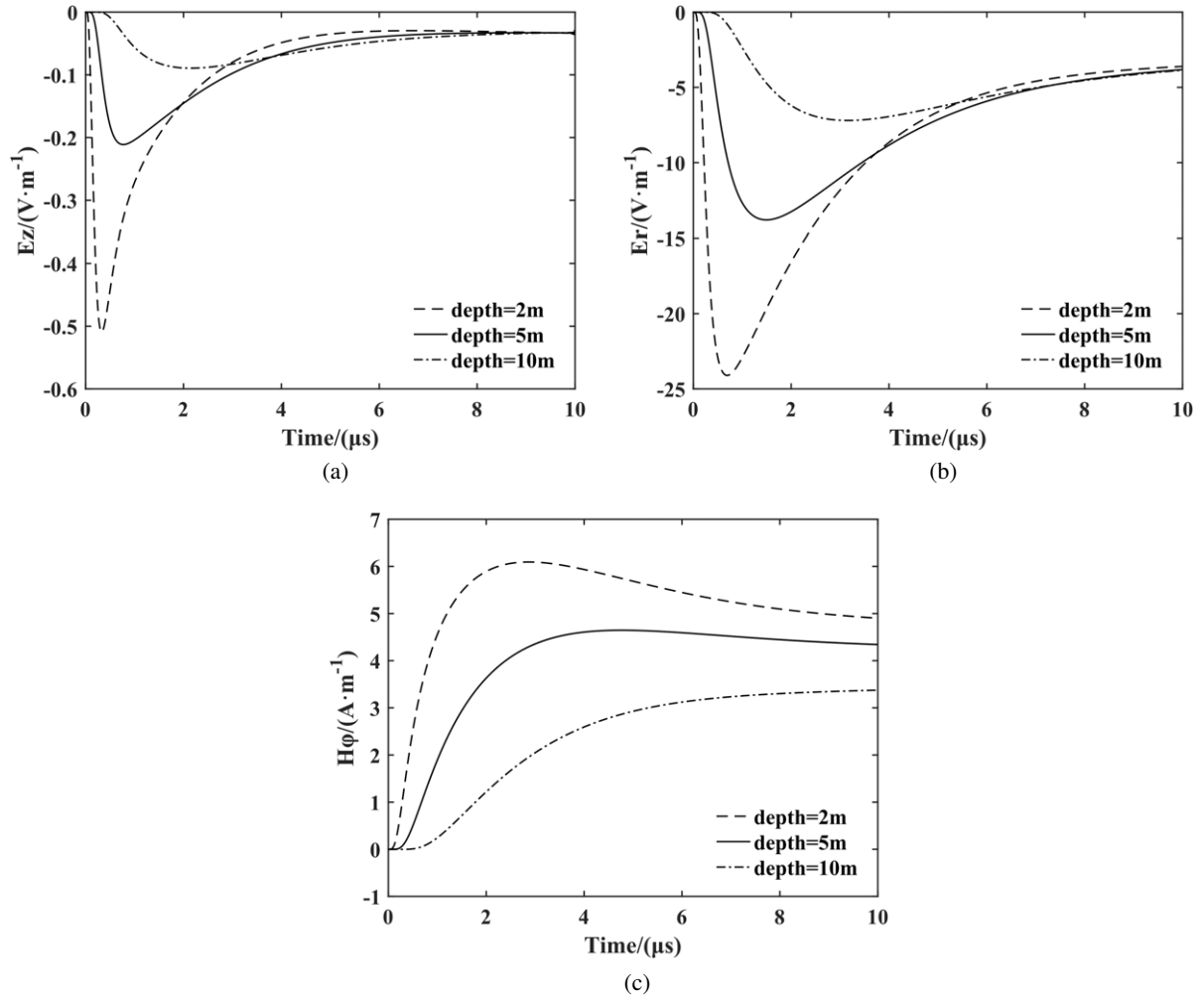


Fig. 4. Electromagnetic field components generated by the lightning return stroke in wet limestone in different depths at a horizontal distance of 200 m, simulated using FDTD method. (a) Vertical electric field, (b) Horizontal electric field, (c) Azimuthal magnetic field.

water content is the most important factor affecting soil conductivity compared to soil surface adsorption effects [22]. Therefore, it is more reasonable to consider soil water content than treating soil conductivity as a constant in order to study propagation of underground electromagnetic fields.

In what follows, the conductivities of clay, silt, and sand in different humidity conditions measured by X. Sun et al. [23] with the forced current method are used in our study. Relationships between conductivity and water content in three soils are determined using linear regression with the following models [23]:

$$\begin{cases} \sigma_{clay} = 0.005727p - 0.02512 \\ \sigma_{silt} = 0.003111p + 0.006215 \\ \sigma_{sand} = 0.001437p - 0.002342. \end{cases} \quad (6)$$

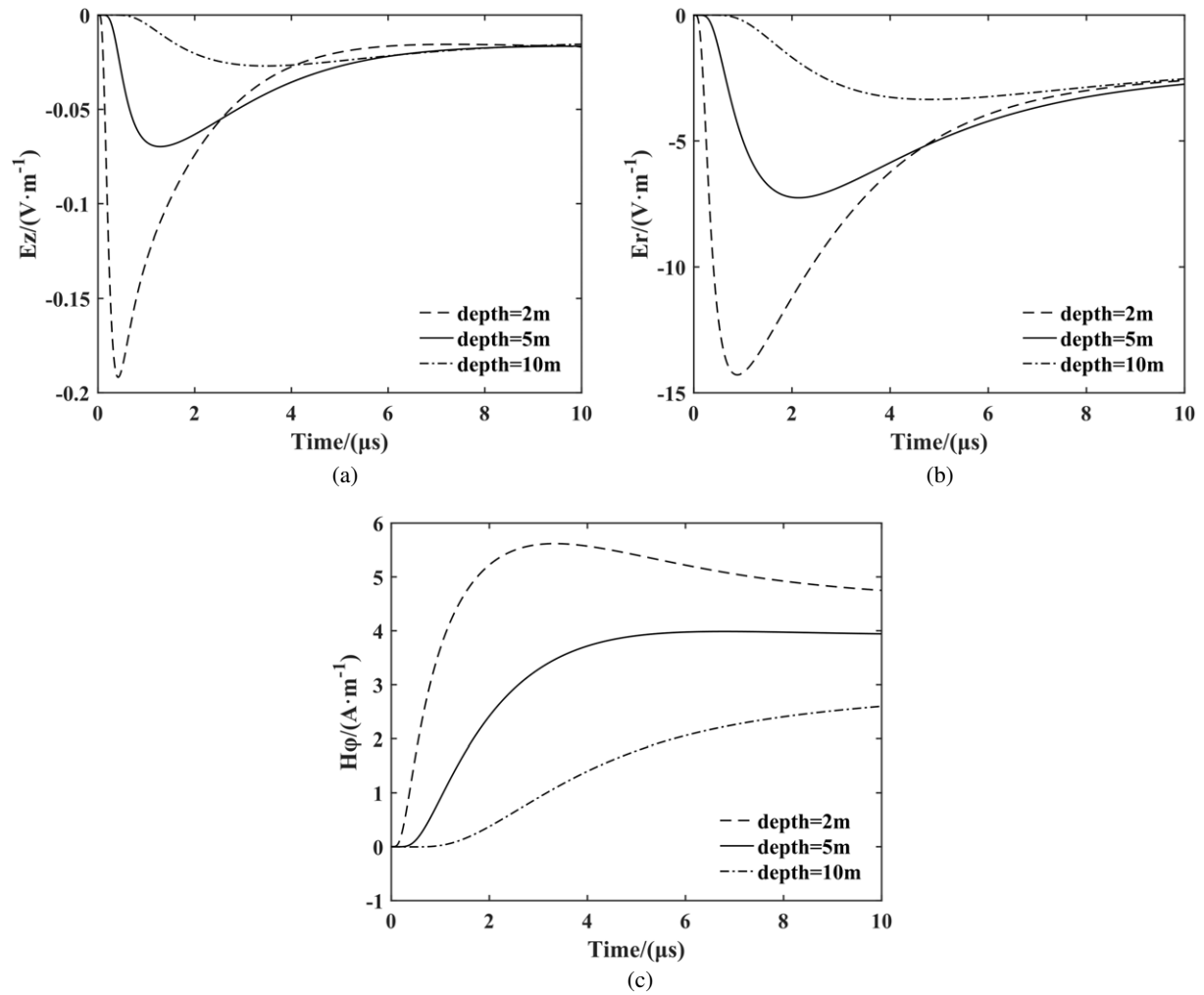


Fig. 5. Electromagnetic field components generated by the lightning return stroke in wet clay in different depths at a horizontal distance of 200 m, simulated using FDTD method. (a) Vertical electric field, (b) Horizontal electric field, (c) Azimuthal magnetic field.

Where,  $p$  is the soil water content and  $\sigma$  is the soil conductivity. Assume soil water content varies from 5% to 25% and the interval is set to 10% in this study. Electromagnetic fields propagating in the three types of soil can be analyzed using FDTD method.

Figures 6–8 show the electromagnetic field components in clay, silt, and sand with 5%, 15%, and 25% water content respectively, generated by the lightning return stroke at a horizontal distance of 200 m in 3 m depth. One can see that changes in water content have the greatest influence on the vertical electric field, followed by the horizontal electric field and the azimuthal magnetic field is least affected, regardless of the type of soil. Because soil is generally a non-magnetic medium, changes in water content have little effect on magnetic properties, and the electrical conductivity increases as the concentration of conductive ions in water, thus attenuation of high-frequency components of the electric field is more obvious. Therefore, water content has a stronger influence on the electric field compared to the magnetic field.



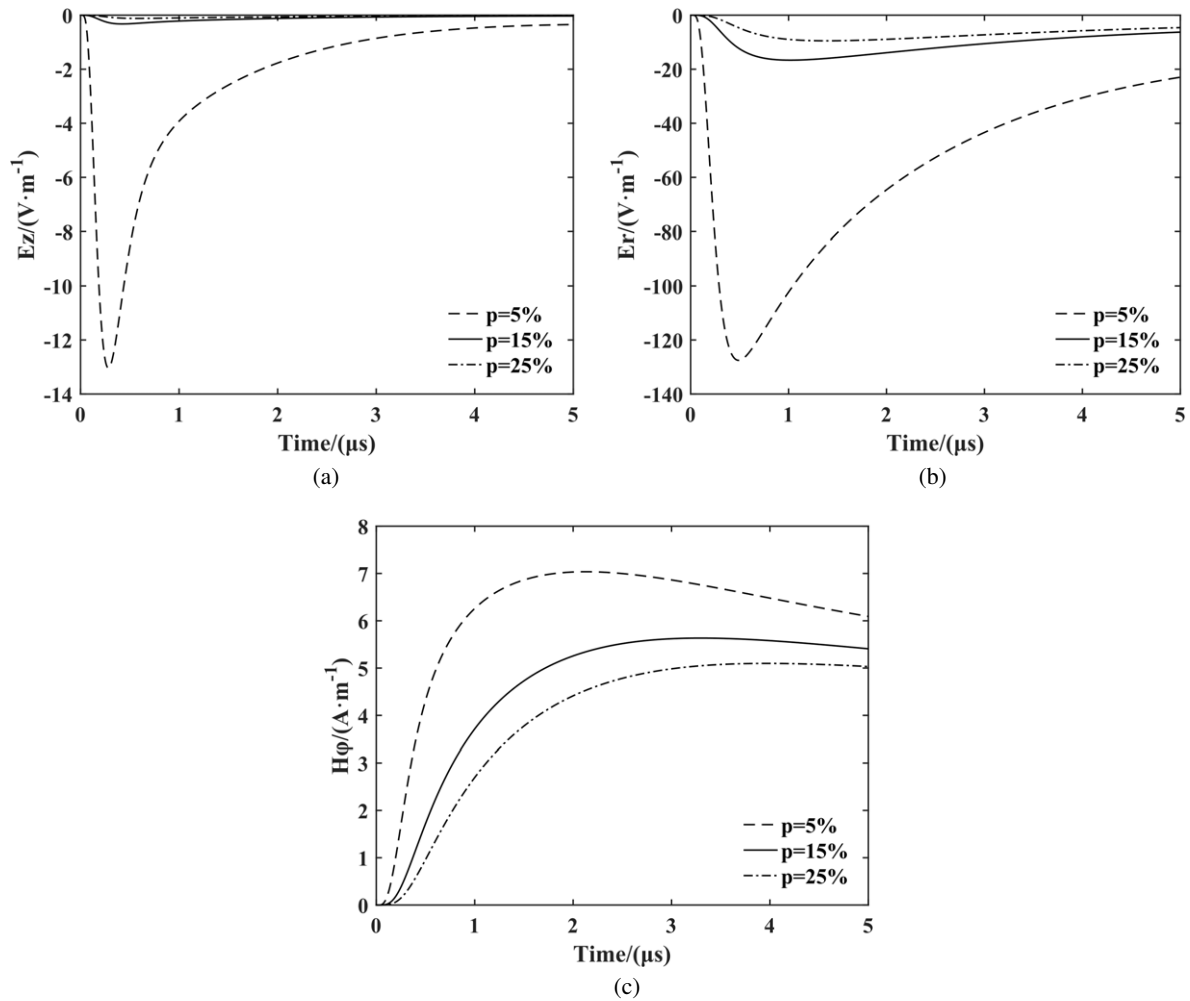


Fig. 6. Electromagnetic field components in clay with different water content in 3 m depth at a horizontal distance of 200 m, simulated using FDTD method. (a) Vertical electric field, (b) Horizontal electric field, (c) Azimuthal magnetic field.

In order to quantitatively describe attenuation of lightning electromagnetic fields in soils with different water content, Tables 3–5 show changes in peak values and rise time of the electromagnetic fields.

In terms of changes in peak values, electromagnetic fields in soil with water content ranging from 5% to 15% will be greatly attenuated. The decay rates of vertical electric fields in each type of soil are 97.5%, 71%, and 82%. Attenuation rates of horizontal electric fields are 86.9%, 49.5%, and 61%. Attenuation rates of azimuthal magnetic fields are 20.3%, 9%, and 8%. In addition to attenuation of peak values, rise time is also obviously delayed.

While, electromagnetic fields will be less attenuated when water content ranges from 15% to 25%, due to the saturation of water in soil pores and stable conductivity. Meanwhile, due to changes in water content, attenuation in clay is greater than that in silt and sand. This is because clay has less sand content, more pores, slower water seepage, and better water retention than silt and sand. Therefore, moisture is a greater determinant of electrical conductivity in clay.

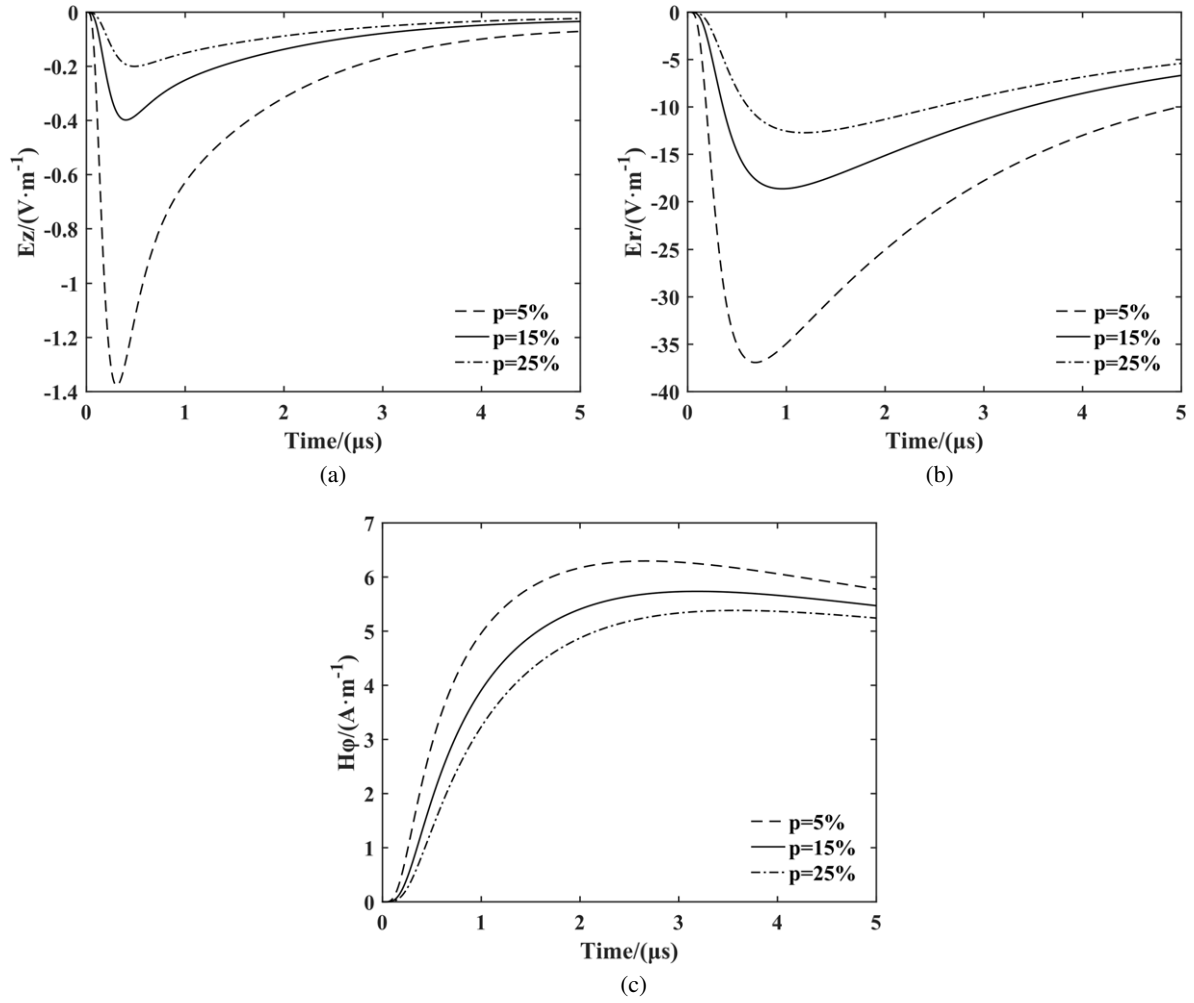


Fig. 7. Electromagnetic field components in silt with different water content in 3 m depth at a horizontal distance of 200 m, simulated using FDTD method. (a) Vertical electric field, (b) Horizontal electric field, (c) Azimuthal magnetic field.

Table 3  
Electromagnetic field peak values and rise time in clay with different water content

Water content	Vertical electric field peak value (V/m)/Rise time ( $\mu\text{s}$ )	Horizontal electric field peak value (V/m)/Rise time ( $\mu\text{s}$ )	Azimuthal magnetic field peak value (V/m)/Rise time ( $\mu\text{s}$ )
$P = 5\%$	-13.03/0.28	-127.53/0.49	7.06/2.35
$P = 15\%$	-0.32/0.42	-16.65/1.02	5.63/3.08
$P = 25\%$	-0.12/0.58	-9.48/1.39	5.06/3.64

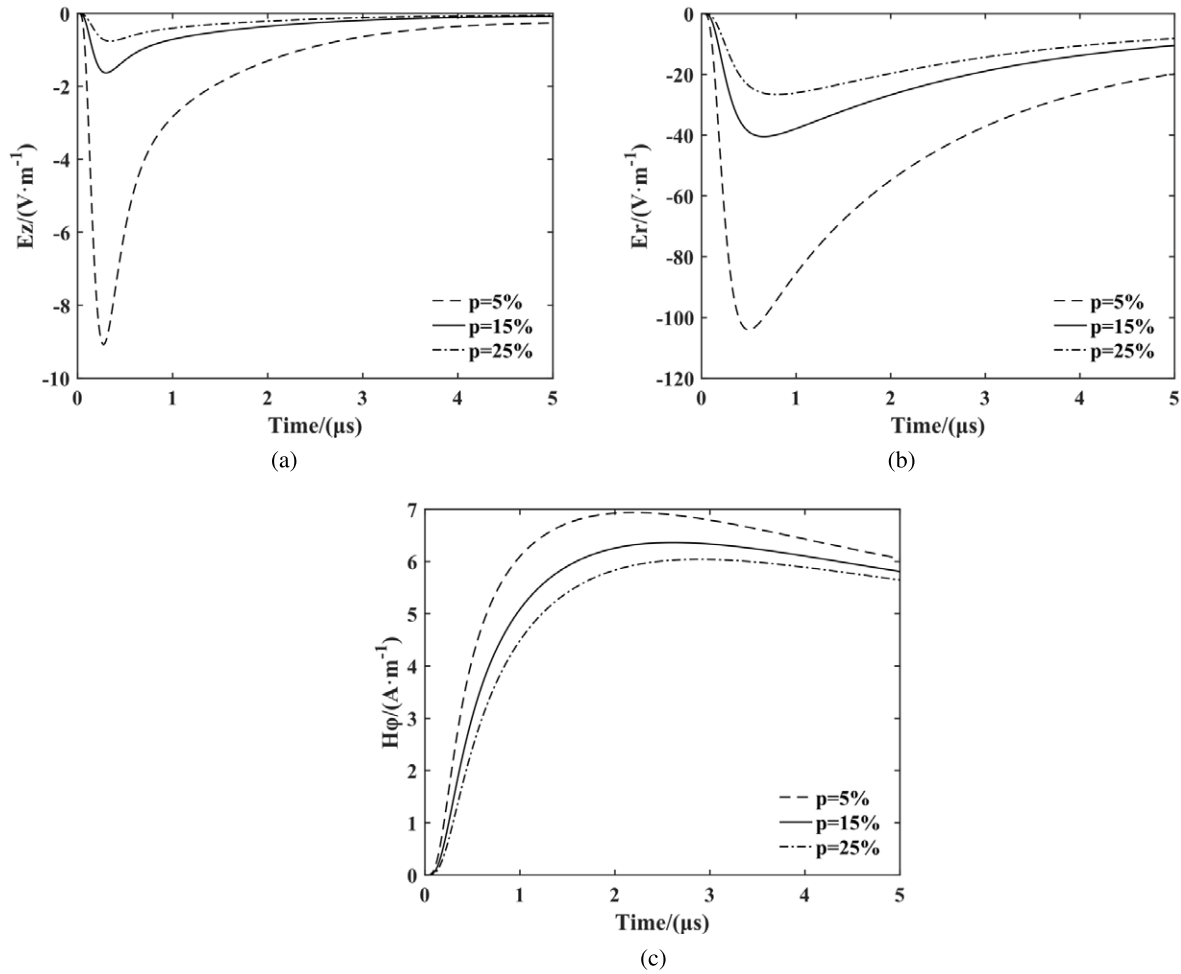


Fig. 8. Electromagnetic field components in sand with different water content in 3 m depth at a horizontal distance of 200 m, simulated using FDTD method. (a) Vertical electric field, (b) Horizontal electric field, (c) Azimuthal magnetic field.

Table 4  
Electromagnetic field peak values and rise time in silt with different water content

Water content	Vertical electric field peak value (V/m)/Rise time (μs)	Horizontal electric field peak value (V/m)/Rise time (μs)	Azimuthal magnetic field peak value (V/m)/Rise time (μs)
$P = 5\%$	-1.38/0.31	-36.92/0.68	6.33/2.60
$P = 15\%$	-0.40/0.40	-18.64/0.96	5.74/2.99
$P = 25\%$	-0.20/0.49	-12.72/1.18	5.36/3.31

## 5. Conclusions

In this paper, we calculated and analyzed propagation effects of underground lightning electromagnetic fields in freshwater, wet limestone, and wet clay in the same horizontal distance and different depths using

Table 5  
Electromagnetic field peak values and rise time in sand with different water content

Water content	Vertical electric field peak value (V/m)/Rise time ( $\mu$ s)	Horizontal electric field peak value (V/m)/Rise time ( $\mu$ s)	Azimuthal magnetic field peak value (V/m)/Rise time ( $\mu$ s)
$P = 5\%$	-9.08/0.27	-104.04/0.50	6.97/2.37
$P = 15\%$	-1.63/0.30	-40.46/0.66	6.39/2.57
$P = 25\%$	-0.76/0.34	-26.64/0.80	6.06/2.76

FDTD method. Attenuation characteristics in clay, silt, and sand with different water content were also analyzed. The following conclusions can be drawn from this paper.

(1) Lightning electromagnetic fields do not change significantly propagating in freshwater in different depths. While in wet limestone and wet clay, attenuation is more obvious with depth.

(2) No matter what geological environment electromagnetic fields propagate, attenuation of electric field is significantly greater than magnetic field, and attenuation of the vertical electric field component is most significant.

(3) Regardless of the type of soil, underground electromagnetic fields have a greater attenuation in soils with water content ranging from 5% to 15%, compared to soils with water content ranging from 15%–25%. Attenuation in clay is the most obvious.

(4) In the geological environments discussed above, the amplitude of the horizontal electric field is greater than that of the vertical electric field and the azimuthal magnetic field. The horizontal electric field may carry the most energy of the underground electric field. Therefore, the induced voltage caused by the horizontal electric field in the protection engineering of underground cables and equipment is not negligible.

## Acknowledgements

This work was supported by the National Key Research and Development Program of China (2017YFC0209603) and Jiangsu Overseas Research & Training Program for University Prominent Young & Middle-aged Teachers and Presidents (2018).

## References

- [1] M. Rubinstein, An approximate formula for the calculation of the horizontal electric field from lightning at close, intermediate, and long range, *IEEE Transactions on Electromagnetic Compatibility* **38**(3) (1996), 531–535, doi:10.1109/15.536087.
- [2] D.A. Hill and J.R. Wait, HF ground wave propagation over mixed land, sea, and sea-ice paths, *IEEE Transactions on Geoscience Remote Sensing* **GE-19**(4) (1981), 210–216, doi:10.1109/TGRS.1981.350374.
- [3] M. Izadi, M.Z.A.A. Kadir, C. Gomes and W.F.W. Ahmad, Numerical expressions in time domain for electromagnetic fields due to lightning channels, *International Journal of Applied Electromagnetics and Mechanics* **37** (2011), 275–289, doi:10.3233/JAE-2011-1400.
- [4] K.S. Yee, Numerical solution of initial boundary value problems involving Maxwell's equations in isotropic media, *IEEE Transactions on Antennas and Propagation* **14**(3) (1966), 302–307, doi:10.1109/TAP.1966.1138693.

- [5] Y. Baba and V.A. Rakov, Applications of the FDTD method to lightning electromagnetic pulse and surge simulations, *IEEE Transactions on Electromagnetic Compatibility* **56**(6) (2014), 1506–1521, doi:10.1109/TEM.2014.2331323.
- [6] M. Boumaiza and D. Labed, Lightning electromagnetic yield coupling to overhead power components lines, *International Journal of Applied Electromagnetics and Mechanics* **47** (2015), 1093–1106, doi:10.3233/JAE-140144.
- [7] K. Arzag, Z. Azzouz, Y. Baba and B. Ghemri, 3D computation of lightning electromagnetic fields in the presence of a horizontally stratified ground, *International Journal of Power and Energy Systems* **37**(4) (2017), 120–128, doi:10.2316/Journal.203.2017.4.203-6284.
- [8] K. Arzag, Z. Azzouz and B. Ghemri, Lightning electric and magnetic fields computation using the 3D-FDTD method and electromagnetic models in presence of different ground configurations, *IEEE transactions on power and energy* **138**(5) (2018), 315–320, doi:10.1541/ieejpes.138.315.
- [9] A. Mimouni, F. Rachidi and M. Rubinstein, Electromagnetic fields of lightning return stroke in presence of stratified ground, *IEEE Transactions on Electromagnetic Compatibility* **56**(2) (2014), 413–418, doi:10.1109/TEM.2013.2282995.
- [10] J. Paknahad, K. Sheshyani, F. Rachidi and M. Paolino, Lightning electromagnetic fields and their induced currents on buried cables. Part II: The effect of a horizontally stratified ground, *IEEE Transactions on Compatibility Electromagnetic* **56**(5) (2014), 1146–1154, doi:10.1109/TEM.2014.2311926.
- [11] A. Taflov and S.C. Hagness, *Computational Electrodynamics: The Finite-Difference Time-Domain Method*, Artech House, Norwood, MA, USA, 2005.
- [12] G. Mur, Absorbing boundary conditions for the finite-difference approximation of the time-domain electromagnetic-field equations, *IEEE Transactions on Electromagnetic Compatibility* **EMC-23**(4) (1981), 377–382, doi:10.1109/TEM.1981.303970.
- [13] F. Rachidi and C.A. Nucci, On the Master, Uman, Lin, Standler and the modified Transmission Line Lightning return stroke current models, *Journal of Geophysical Research* **95**(D12) (1990), 20389, doi:10.1029/jd095id12p20389.
- [14] Y. Baba and V.A. Rakov, On the transmission line model for lightning return stroke representation, *Geophysical Research Letters* **30**(24) (2003), 2294, doi:10.1029/2003GL018407.
- [15] G. Diendorfer and M.A. Uman, An improved return stroke model with specified channel-base current, *Journal of Geophysical Research-Atmospheres* **95**(D9) (1990), 13621–13644, doi:10.1029/jd095id09p13621.
- [16] F. Rachidi, W. Janischewskyj, A.M. Hussein, C.A. Nucci, S. Guerrieri, B. Kordi and J.S. Chang, Current and electromagnetic field associated with lightning-return strokes to tall towers, *IEEE Transactions on Electromagnetic Compatibility* **43**(3) (2001), 356–367, doi:10.1109/15.942607.
- [17] V. Cooray, Underground electromagnetic fields generated by the return strokes of lightning flashes, *IEEE Transactions on Electromagnetic Compatibility* **43**(1) (2001), 75–84, doi:10.1109/15.917942.
- [18] F. Delfino, R. Procopio, M. Rossi, F. Rachidi and C.A. Nucci, An algorithm for the exact evaluation of the underground lightning electromagnetic fields, *IEEE Transactions on Electromagnetic Compatibility* **49**(2) (2007), 401–411, doi:10.1109/TEM.2007.897127.
- [19] A. Mimouni, F. Delfino, R. Procopio and F. Rachidi, On the computation of underground electromagnetic fields generated by lightning: a comparison between different approaches, *IEEE Lausanne Power Tech* (2008), doi:10.1109/PCT.2007.4538413.
- [20] G.W. Han, T.Y. Wang, B. Liu and L.J. Wang, Geological radar forecasting and detection of tunnel diseases, *Survey Science and Technology* **2** (2007), 58–61.
- [21] F.S. Zha and S.Y. Liu, Discussion on the theory of resistivity of soil and its application, *Geotechnical Investigation and Surveying* **5** (2006), 10–15.
- [22] D.W. Zhang, Z.G. Cao and S.Y. Liu, Change law and empirical model of resistivity of solidified soil, *Journal of Rock Mechanics and Engineering* **33**(z2) (2014), 4139–4144.
- [23] X. Sun, Q.Y. Yang, L. Gao and Z.Y. Li, Study on the effect of humidity change on soil resistivity, *Geotechnical Investigation and Surveying* **47**(01) (2019), 39–44.